Differentiation of affected and nonaffected ovaries in ovarian torsion with magnetic resonance imaging texture analysis

Tumay Bekci[1]* , Ismet Mirac Cakir[1] , Serdar Aslan[1]

SUMMARY

OBJECTIVE: This study aimed to evaluate the feasibility of texture analysis on T2-weighted axial images in differentiating affected and nonaffected ovaries in ovarian torsion.

METHODS: We included 22 torsioned ovaries and 19 healthy ovaries. All patients were surgically proven ovarian torsion cases. On T2-weighted axial images, ovarian borders were delineated by the consensus of two radiologists for magnetic resonance imaging-based texture analysis. Statistical differences between texture features of affected and nonaffected ovaries were assessed.

RESULTS: A total of 44 texture features were extracted from each ovary using LIFEx software. Of these, 17 features were significantly different between affected and nonaffected ovaries in ovarian torsion. NGLDM_Coarseness and NGLDM_Contrast, which are the neighborhood gray-level difference matrix parameters, had the largest area under the curve: 0.923. The best cutoff values for the NGLDM_Contrast and NGLDM_Coarseness were 0.45 and 0.01, respectively. With these cutoff levels, NGLDM_Contrast had the best accuracy (85.37%).

CONCLUSION: Magnetic resonance imaging-based texture analysis on axial T2-weighted images may help differentiate affected and nonaffected ovaries in ovarian torsion.

KEYWORDS: Artificial intelligence. Diagnostic techniques. Obstetrical and gynecological.

INTRODUCTION

Ovarian torsion (OT) is defined as a partial or complete turn of the ovary and ovarian vascular pedicle on its long axis[1,2]. OT results venous blood flow obstruction, edema, and consequent necrosis of ovarian tissue because of subsequent arterial blood flow obstruction[2]. Its nonspecific symptoms and a wide differential diagnosis of pelvic abdominal pain make it difficult to diagnose OT, even in experienced hands, with the use of multimodality screening tools. Furthermore, the reliability of ultrasonography (US) and magnetic resonance imaging (MRI) assessments in the diagnosis of OT is limited by the variety of experience of radiologists[1,2]. An increased incidence of OT, especially in pregnant women, children, and women undergoing ovulation induction therapy, draws attention to this issue[1]. In contrast, timely diagnosis and management of OT is crucial for the preservation of ovarian reserve and fertility[1]. Thus, an accurate, noninvasive method that does not use contrast media or radiation to predict OT preoperatively is essential for the overall treatment of OT, especially in children and pregnant women.

Texture analysis (TA) is an emerging technique that allows for the analysis of the distribution of pixel intensities and transforms digital medical images into mineable data by extracting quantitative features mathematically[3-18]. TA has recently been investigated for the identification of brain, renal, lung, and ovarian tumors and diseases[6,8]. However, to the best of our knowledge, there is still no study in the literature that uses TA to differentiate affected and nonaffected ovaries in OT. TA is a promising method, and the texture data obtained can be used in deep learning algorithms for rapid diagnosis and treatment of OT in emergency settings. The most obvious example of this is artificial intelligence-based algorithms used in stroke patients[19]. OT, in contrast, is a difficult process to diagnose, and the fact that the torsed and nontorsed ovaries can be differentiated by TA can provide rapid diagnosis and treatment of OT with deep learning applications in emergency settings. We think that TA may help differentiate affected and nonaffected ovaries based on lesion signal intensity characteristics in MRI. Accordingly, we aimed to investigate the feasibility and accuracy of TA for differentiating affected and nonaffected ovaries in OT on T2-weighted MR images.

METHODS

A flowchart of the TA model is shown in Figure 1.

Patients

This retrospective study was approved by the institutional review board of our university hospital, and written informed consent was waived (OMU/KAEK-2016/49). The database of our university hospital was reviewed to identify surgically proven OT patients with preoperative MRI examinations between January 2015 and April 2020. The inclusion criteria were surgically proven OT, MRI examination prior to surgery, and having an axial T2-weighted MRI (n=22). The exclusion criterion was MR images with motion artifacts (n=1) and torsion cases with paraovarian cysts neoplasms (n=3).

MR image acquisition and ovarian segmentation

A 1.5-T MRI Scanner (Siemens Magnetom Symphony Quantum, Erlangen, Germany) equipped with phased-array coils was used for MRI examinations. The standard T2-weighted MRI protocol was used.

The affected and nonaffected ovaries were manually segmented by the consensus of two radiologists with 9 and 8 years of experience in abdominal imaging using LIFEx software (www.lifex-soft.org). LIFEx software is a free, multiplatform, and easy-to-use freeware called LIFEx, which enables the calculation of conventional, histogram-based, textural, and shape features from PET, SPECT, MR, CT, and US images, or from any combination of imaging modalities. Axial T2-weighted MR images were exported in Digital Imaging and Communications in Medicine (DICOM) format from the hospital database to LIFEx software. The region of interest included the largest cross-sectional, two-dimensional area of ovaries in axial planes selected on T2-weighted MR images (Figure 2)[16]. All ovarian tissue was used, including cysts and necrosis. Paraovarian cysts neoplasms, which cause some adnexal torsion cases, were excluded (n=3). After ovarian segmentation, texture feature extraction was performed.

Texture feature extraction

Texture analysis was obtained from two-dimensional images of segmented ovaries on axial plain using LIFEx software. Preprocessing steps including spatial resampling, gray-level discretization, and intensity rescaling were performed for all MR images after ovarian segmentation. To create homogeneity for the voxel values, spatial resampling was performed, and after calculating their means±standard deviations, *X-Y-Z* directions
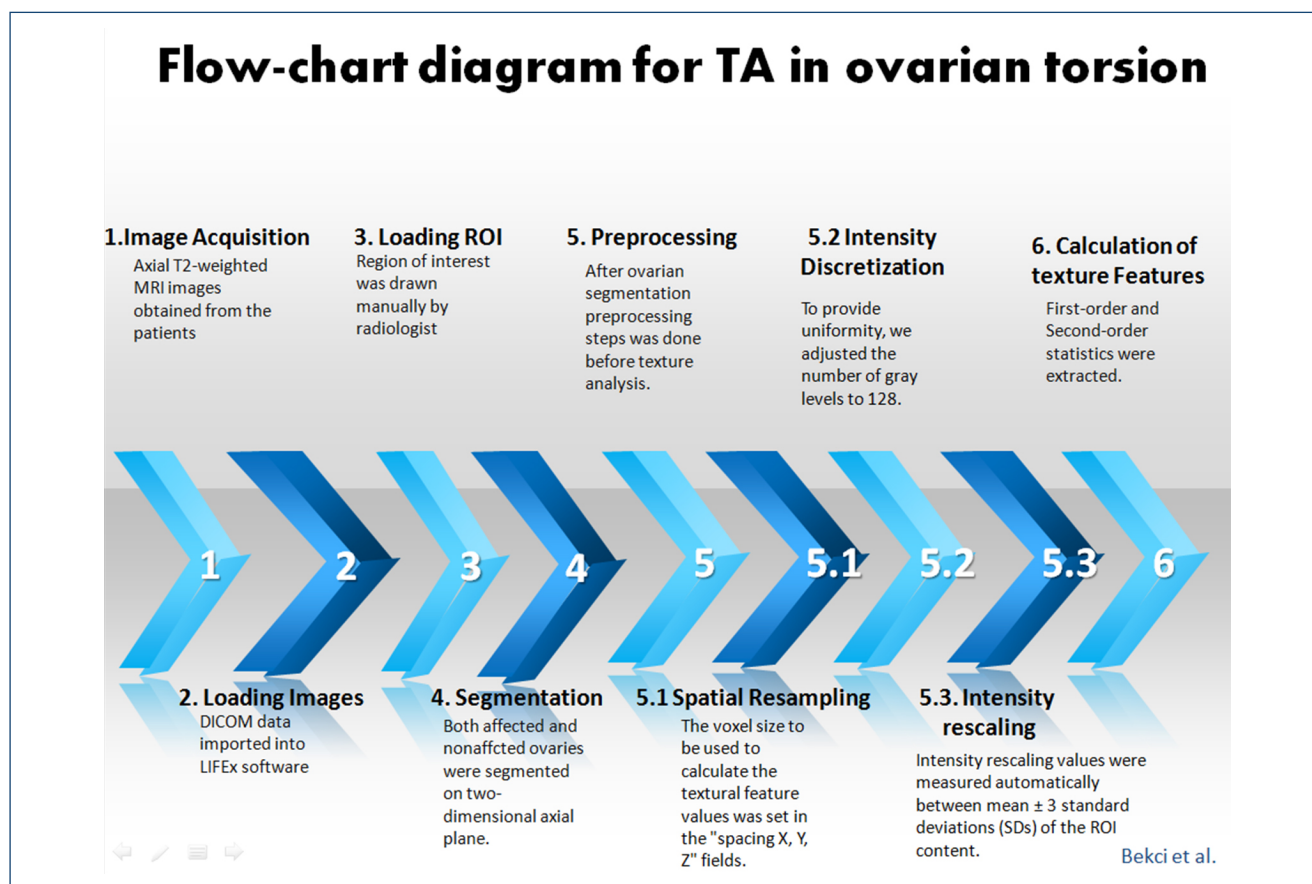

Figure 1. Flowchart diagram for texture analysis in ovarian torsion.

were rescaled as 0.87, 1.07, and 5, respectively. A gray-level range between 1 and 128 bits/pixel was used for intensity discretization to ensure uniformity for TA. The ±3 sigma technique was used for intensity rescaling to minimize different MRI protocol effects. A total of 44 texture features were extracted. Notably, 12 first-order features were derived from discretized, conventional, histogram, and shape features, and 32 second-order features were derived from gray-level co-occurrence matrix (GLCM) features, gray-level run-length matrix (GLRLM) features, neighborhood gray-level different matrix (NGLDM) features, and gray-level zone length matrix (GLZLM) features.

Statistical analysis

Statistical analyses were performed using IBM SPSS version 23. Normality distributions of quantitative parameters were analyzed using the Shapiro-Wilk test. The Mann-Whitney U test was used to compare data that did not conform to normal distributions. Receiver operator characteristic (ROC) analysis was performed for diagnostic test evaluation, and sensitivity and specificity were evaluated. Data are expressed as mean (95% confidence interval). A $p<0.05$ was considered statistically significant.

In the power analysis performed with reference to the results of the Bekci et al.'s study, which is evaluated diffusion-weighted MRI features of torsioned and normal ovaries, with a test power to be 95%, a total of 22 cases are required, with 11 cases in each group[20].

RESULTS

Patient characteristics

The median age of the patients was 27 (range 5–65). In all, 26 surgically proven OT patients were evaluated. A total of 41 ovaries were included in the study in 22 patients, excluding the cases with motion artifact (n=1) and paraovarian cyst neoplasm (n=3), which were the exclusion criteria. Three OT patients had previous oophorectomy. A total of 22 torsioned ovaries and 19 healthy ovaries were evaluated.

Texture features

A total of 1 first-order and 16 second-order features, including 1 DISCRETIZED_HISTO_Entropy_log2 feature, 5 GLCM features, 4 GLRLM features, 3 NGLDM features, and 4 GLZM features, demonstrated statistically significant difference between affected and nonaffected ovaries on T2-weighted axial MR images in OT patients. NGLDM_Coarseness and NGLDM_Contrast, which are the NGLDM parameters, had the largest area under the curve: 0.923 (Figure 3). The best cut-off values for NGLDM_Contrast and NGLDM_Coarseness were 0.45 and 0.01, respectively. With these threshold values, sensitivity, specificity, and accuracy values were 86.36% (65.09–97.09%), 84.21% (60.42–96.62%), 85.37% and 36.36% (17.2–59.34%), 100% (82.35–100%), and 65%, respectively. NGLDM_Contrast had the best accuracy (85.37%).

DISCUSSION

Magnetic resonance imaging-based TA analysis on T2-weighted axial images for the differentiation of affected and nonaffected ovaries in OT was investigated in this study for the first time in the medical literature. A total of 17 TA features were significantly different between affected and nonaffected ovaries, with ROC values ranging between 0.679 and 0.923. Our results demonstrate that NGLDM_Contrast, which is the NGLDM parameter, has excellent differentiation accuracy, with an area under curve (AUC) of 0.923 for affected and nonaffected ovaries
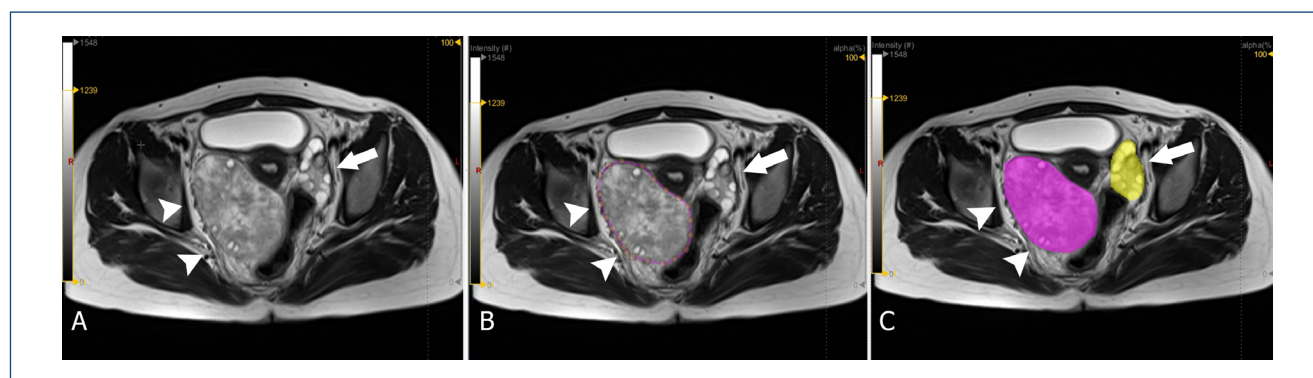
Figure 2. (A) 30-year-old women with right-sided surgically proven ovarian torsion. T2-weighted axial magnetic resonance imaging demonstrate enlarged right ovary with peripherally located cysts [arrowheads]. Arrow indicates normal ovary on the left. **(B)** The region of interest included the largest cross-sectional, two-dimensional area [arrowheads] of ovary in axial plane selected on T2-weighted magnetic resonance imaging. **(C)** Both affected [arrowheads] and nonaffected ovaries [affected] manually segmented by the consensus of two radiologists using LIFEx software.

in OT. NGLDM_Coarseness and NGLDM_Contrast values of 0.45 and 0.01 were the best diagnostic parameters for predicting OT, respectively. With these threshold values, sensitivity and specificity reached 86.36% and 100%, respectively.

Ovarian torsion is increasingly prevalent, especially in children and pregnant women[2]. Although US is the first choice of imaging modality used in the diagnosis of OT, for further investigation, MRI is used as an advanced imaging method in most cases[1,2]. However, both the user-dependent diagnostic performance of US and the varying accuracy of MRI have required the development of a new method for the diagnosis of OT[1]. In addition, the need for the use of contrast agents during the classical evaluation of OT with MRI presents a disadvantage for pediatric cases and pregnant women. At this point, TA plays an important role in the diagnosis of OT without using contrast media or radiation exposure.

Texture analysis is a mathematical method that allows the examination of changes in intensity that cannot be detected with the human eye in MR images[9-12]. Texture features can be divided into five groups: size- and shape-based features, descriptors of the image intensity histogram, descriptors of the relationships between image voxels (e.g., GLCM features, GLRLM features, NGLDM features, and GLZLM features), and fractal features[13]. We used TA only on axial T2-weighted images. Using only a single MRI sequence for MRI examination is essential in terms of time management, which is important in the diagnosis and treatment of OT. After careful segmentation of ovaries by the consensus of two radiologists, texture features were extracted. Our study demonstrated that 17 parameters consisting of first- and second-order features differ significantly with TA of axial T2-weighted images. Of these, NGLDM_Contrast, which is a second-order feature, was able to predict torsed ovaries with the highest accuracy. A neighboring gray tone difference matrix quantified the difference between a gray value and the average gray value of its neighbors within distance[3,4]. Contrast is a measure of a spatial intensity change, but it is also dependent on the overall gray-level dynamic range[15,17,21]. Contrast is high when both the dynamic range and the spatial change rate are high, i.e., an image with a large range of gray levels, with large changes between voxels and their neighborhood[15,21]. From a mathematical point of view, NGLDM_Contrast reflects how much the gray levels of neighboring regions differ[15,21]. In our
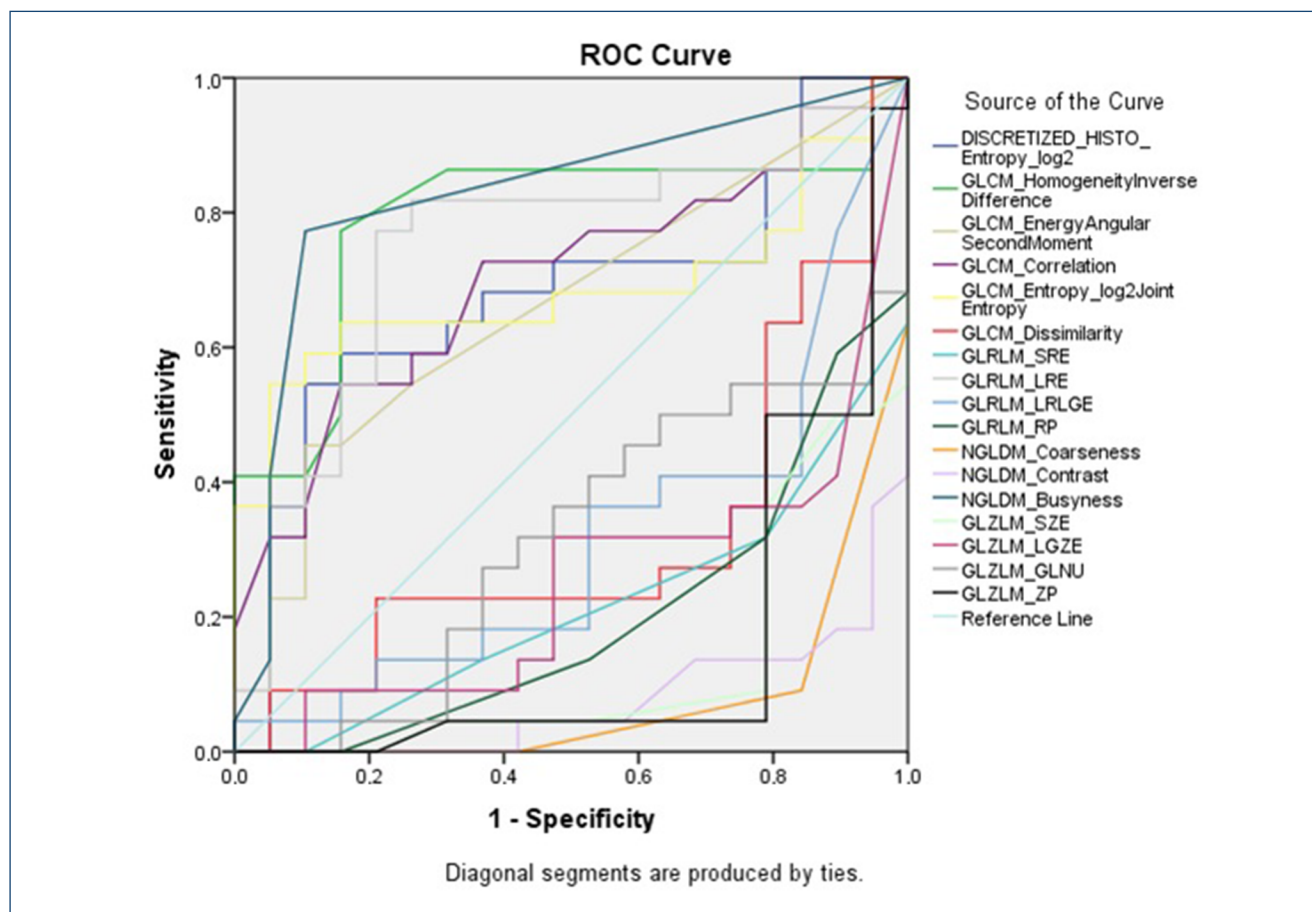

Figure 3. Receiver-operating characteristics curve of texture analysis parameters for differentiating affected ovary from nonaffected ovary.

study, torsioned ovaries showed lower contrast. We could, therefore, hypothesize that OT presents a more homogeneous parenchymal texture. This may be associated with edema caused by venous congestion in the torsed ovaries. Edema caused by congestion develops in almost all torsed ovaries, and this finding is consistent with the pathophysiological and morphological features of OT.

This study has some limitations. The first limitation is the relatively small number of cases examined. Second, we used only T2-weighted images for TA. Using or combining other MRI sequences, such as contrast-enhanced or diffusion-weighted images, may expand the feature pool and improve the diagnostic performance of texture features. Additionally, combining conventional features with texture features and to calculate added value might be useful. Third, we did not study interobserver agreement to test the reproducibility of the method. In the future, it is necessary to study using multisequence texture features and conventional features of OT with larger samples.

CONCLUSIONS

Our study results show that MRI-based TA can be used to differentiate affected and nonaffected ovaries in OT. A set of parameters, especially NGLDM_Contrast, can predict torsioned ovaries with high accuracy. By implementing the defined parameter with high diagnostic accuracy into artificial intelligence applications, early diagnosis and treatment of OT can be enabled in emergency settings. The data we obtained in our study should be supported by new studies and the feasibility of using it in the diagnosis of OT should be evaluated by using it in artificial intelligence applications in further studies. TA may be an important part of diagnosis of OT in daily practice.

ETHICAL CONSIDERATIONS

This study was approved by the Ethics Committee of our hospital. Due to the prospective nature of the study, informed consent for prospective data analysis was taken by the institutional review board.

AUTHORS' CONTRIBUTIONS

TB: Conceptualization, Writing – original draft. **IMC:** Data curation, Formal Analysis. **SA:** Formal Analysis, Writing – review & editing.

REFERENCES

1. Sintim-Damoa A, Majmudar AS, Cohen HL, Parvey LS. Pediatric ovarian torsion: spectrum of imaging findings. Radiographics. 2017;37(6):1892-908. https://doi.org/10.1148/rg.2017170026

2. Gounder S, Strudwick M. Multimodality imaging review for suspected ovarian torsion cases in children. Radiography. 2021;27(1):236-42. https://doi.org/10.1016/j.radi.2020.07.006

3. Sarioglu O, Sarioglu FC, Akdogan AI, Kucuk U, Arslan IB, Cukurova I, et al. MRI-based texture analysis to differentiate the most common parotid tumours. Clin Radiol. 2020;75(11):877-e15. https://doi.org/10.1016/j.crad.2020.06.018

4. Sarioglu O, Sarioglu FC, Capar AE, Sokmez DFB, Topkaya P, Belet U. The role of CT texture analysis in predicting the clinical outcomes of acute ischemic stroke patients undergoing mechanical thrombectomy. Eur Radiol. 2021;31(8):6105-15. https://doi.org/10.1007/s00330-021-07720-4

5. Sarioglu FC, Sarioglu O, Guleryuz H, Ozer E, Ince D, Olgun HN. MRI-based texture analysis for differentiating pediatric craniofacial rhabdomyosarcoma from infantile hemangioma. Eur Radiol. 2020;30(10):5227-36. https://doi.org/10.1007/s00330-020-06908-4

6. Zhang S, Chiang GCY, Magge RS, Fine HA, Ramakrishna R, Chang EW, et al. Texture analysis on conventional MRI images accurately predicts early malignant transformation of low-grade gliomas. Eur Radiol. 2019;29(6):2751-9. https://doi.org/10.1007/s00330-018-5921-1

7. Sandrasegaran K, Lin Y, Asare-Sawiri, Taiyini T, Tann M. CT texture analysis of pancreatic cancer. Eur Radiol. 2019;29(3):1067-73. https://doi.org/10.1007/s00330-018-5662-1

8. Kocak B, Durmaz ES, Kaya OK, Kilickesmez O. Machine learning-based unenhanced CT texture analysis for predicting BAP1 mutation status of clear cell renal cell carcinomas. Acta Radiol. 2020;61(6):856-64. https://doi.org/10.1177/0284185119881742

9. Koçak B, Durmaz EŞ, Ateş E, Kılıçkesmez Ö. Radiomics with artificial intelligence: a practical guide for beginners. Diagn Interv Radiol. 2019:25(6);485-95. https://doi.org/10.5152/dir.2019.19321

10. Kocak B, Durmaz ES, Ates E, Ulusan MB. Radiogenomics in clear cell renal cell carcinoma: machine learning–based high-dimensional quantitative CT texture analysis in predicting PBRM1 mutation status. Am J Roentgenol. 2019;212(3):55-63. https://doi.org/10.2214/AJR.18.20443

11. Kocak, B, Durmaz ES, Kadioglu P, Polat Korkmaz O, Comunoglu N, Tanriover N, et al. Predicting response to somatostatin analogues in acromegaly: machine learning-based high-dimensional quantitative texture analysis on T2-weighted MRI. Eur Radiol. 2019;29(6):2731-9. https://doi.org/10.1007/s00330-018-5876-2

12. Zeynalova A, Kocak B, Durmaz ES, Comunoglu N, Ozcan K, Ozcan G, et al. Preoperative evaluation of tumour consistency in pituitary macroadenomas: a machine learning-based histogram analysis on conventional T2-weighted MRI. Neuroradiology. 2019;61(7):767-74. https://doi.org/10.1007/s00234-019-02211-2

13. Koçak B. Reliability of 2D magnetic resonance ımaging texture analysis in cerebral gliomas: ınfluence of slice selection bias on reproducibility of radiomic features. Istanb Med J. 2019;20(5):413-7. https://doi.org/10.4274/imj.galenos.2019.09582

14. Basara Akin I, Ozgul H, Simsek K, Altay C, Secil M, Balci P. Texture analysis of ultrasound images to differentiate simple fibroadenomas from complex fibroadenomas and benign phyllodes tumors. J Ultrasound Med. 2020;39(10):1993-2003. https://doi.org/10.1002/jum.15304

15. Li Z, Mao Y, Huang W, Li H, Zhu J, Li W, et al. Texture-based classification of different single liver lesion based on SPAIR T2W MRI images. BMC Med Imaging. 2017;17:1-9. https://doi.org/10.1186/s12880-017-0212-x

16. Ng F, Kozarski R, Ganeshan B, Goh V. Assessment of tumor heterogeneity by CT texture analysis: can the largest cross-sectional area be used as an alternative to whole tumor analysis? Eur J Radiol. 2013;82(2):342-8. https://doi.org/10.1016/j.ejrad.2012.10.023

17. Varghese BA, Cen SY, Hwang DH, Duddalwar VA. Texture analysis of imaging: what radiologists need to know. Am J Roentgenol. 2019;212(3):520-8. https://doi.org/10.2214/AJR.18.20624

18. Collewet G, Strzelecki M, Mariette F. Influence of MRI acquisition protocols and image intensity normalization methods on texture classification. Magn Reson Imaging. 2004;22(1):81-91. https://doi.org/10.1016/j.mri.2003.09.001

19. Kauw F, Heit JJ, Martin BW, van Ommen F, Kappelle LJ, Velthuis BK, et al. Computed tomography perfusion data for acute ischemic stroke evaluation using rapid software: pitfalls of automated postprocessing. J Comput Assist Tomogr. 2020;44(1):75-7. https://doi.org/10.1097/RCT.0000000000000946

20. Bekci T, Polat AV, Aslan K, Tomak L, Ceyhan Bilgici M, Danaci M. Diagnostic performance of diffusion-weighted MRI in the diagnosis of ovarian torsion: comparison of torsed and nonaffected ovaries. Clin Imaging. 2016;40(5):1029-33. https://doi.org/10.1016/j.clinimag.2016.06.003

21. Pyradiomics Community. Radiomic features; 2016. Available from: https://pyradiomics.readthedocs.io/en/latest/features.html [Accessed 24th February 2021].